NANO LETTERS

2007
Vol. 7, No. 9
2718−2723

Nanowire-Based Delivery of *Escherichia coli* O157 Shiga Toxin 1 A Subunit into Human and Bovine Cells

Nam Hoon Kwon,[†,‡,||] Miles F. Beaux II,[†,§] Chad Ebert,[§] Lidong Wang,[§] Brian E. Lassiter,[§] Yong Ho Park,[||] David N. McIlroy,[†,§] Carolyn J. Hovde,[†,‡] and Gregory A. Bohach*[,†,‡]

Department of Microbiology, Molecular Biology and Biochemistry and Department of Physics, University of Idaho, Moscow, Idaho 83844, and Department of Microbiology, College of Veterinary Medicine, and BK21 Program for Veterinary Science, Seoul National University, Seoul 151-742, Korea

Received May 18, 2007; Revised Manuscript Received July 10, 2007

ABSTRACT

Silica nanowires (NWs) were used to introduce the Shiga toxin type 1 A subunit (StxA1) into cultured bovine and human epithelial cells. We extended technology developed in our laboratories that employs fibronectin (Fn) to induce integrin-mediated uptake of NWs by coating NWs with StxA1 and Fn. The bonding strengths of Fn and StxA1 to the surface of NWs were measured by X-ray photoelectron spectroscopy. This technique demonstrated complex interactions between Fn, StxA1, and the NWs. Neutral red cytotoxicity assays and field emission scanning electron microscopy confirmed that the NW−StxA1−Fn complexes were effectively internalized and caused cell death. This indicates that NWs can carry StxA1 and potentially other toxic or therapeutic agents into eukaryotic cells. Ongoing studies include improved functionalizing of NWs aimed at increasing internalization efficiency and substituting ligands for specific cell targeting.

There is great interest in developing nanomaterials (NMs) to deliver therapeutic agents to cells. Their size may permit NMs to carry drugs across physiological barriers such as the blood−brain barrier, the branching pulmonary pathway, and the tight epithelial junctions that can impede delivery and targeting of drugs.[1,2] Also, NMs may penetrate tumors due to increased vasculature permeability.[3,4] Other merits of NMs are their large surface which can be altered to promote targeting, biocompatibility, solubility, and controlled drug release.[1,2] Thus, NMs could deliver drugs to cells or organelles with relatively low doses and reduced toxicity.[1,2,5] Examples include delivery of insulin, calcitonin, cyclosporin A, dalargin, and anticancer agents such as gelatin−doxorubicin or squalenoyl gemcitabine which have been encapsulated in polymeric organic NMs.[6,7]

Strategies have been developed to functionalize NM surfaces.[2,8−11] Examples include use of surfactants, polymers, oxidation, metals, or biological compounds to enhance NM solubility, targeting efficiency, and delivery into eukaryotic cells.[3,5,9] We previously used fibronectin (Fn) as a molecular bridge to induce integrin-dependent nanowire (NW) internalization by bovine mammary epithelial cells (MAC-T).[12] Fn-induced internalization depends upon endocytosis mediated by $\alpha_5\beta_1$ integrins, key cell membrane Fn receptors.[13] In the present study, Fn-coated NWs delivered recombinant Shiga toxin type 1 (Stx1) A subunit (StxA1) into cultured human laryngeal epithelial cells (HEp-2)[14] and MAC-T cells. Stx1 is an AB_5 toxin, comprised of one A (toxic) subunit and five identical B (receptor binding) subunits. The AB_5 holotoxin is produced by some *Escherichia coli* strains and related to a *Shigella dysenteriae* homologue.[15−17] Stx1 mediates *E. coli* hemorrhagic colitis and the hemolytic uremic syndrome. These food-borne zoonoses are linked to consuming bovine-contaminated food. Also, Stx1 is a biosecurity agent related to ricin.[18,19] Stx1 B subunits bind globotriaosylceramide (Gb_3) receptors on eukaryotic cells and the Stx1 holotoxin enters the cell by receptor-mediated endocytosis. The toxin is transported retrograde through the trans-golgi network to the endoplasmic reticulum where StxA1 subunits are transferred to the cytosol and its ribosomal substrates.[16,20] StxA1 is an *N*-glycosidase that removes an adenine from 28S rRNA, rendering the ribosome unable to undergo protein synthesis.[16] We used recombinant StxA1 which cannot naturally enter cells without its counterpart B subunits.

* Corresponding author: tel, 208-885-6666; fax, 208-885-6654; e-mail, gbohach@uidaho.edu.
† Contributed equally.
‡ Department of Microbiology, Molecular Biology and Biochemistry, University of Idaho.
§ Department of Physics, University of Idaho.
|| Department of Microbiology, College of Veterinary Medicine, and BK21 Program for Veterinary Science, Seoul National University.

10.1021/nl071179f CCC: $37.00
Published on Web 07/27/2007

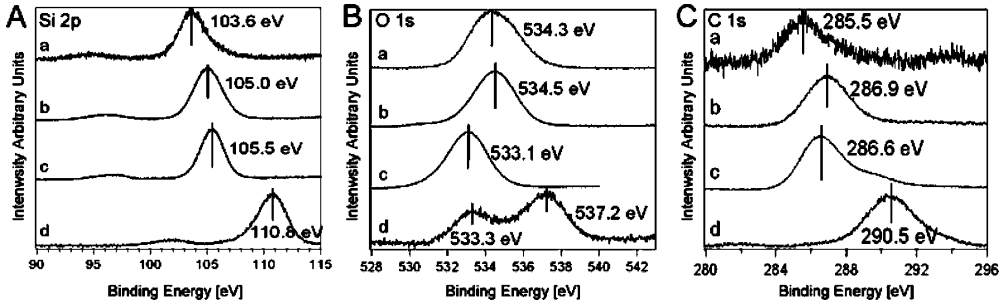

Figure 1. XPS spectra of NW, NW−Fn, or NW-StxA1-Fn complexes: (A) Si 2p spectra; (B) O 1s spectra; (C) C 1s spectra. Energy levels of (a) noncoated NWs, (b) NWs coated with StxA1 only, (c) NWs coated first with StxA1 and then with Fn, and (d) NWs coated simultaneously with Fn and StxA1.

Silica NWs were grown via the vapor−liquid−solid mechanism[21] on Si(100) substrates sputtered with iron as a catalyst, in a Lindberg/Blue three zone programmable tube furnace. High-purity Si powder (99.999%) was placed in an alumina boat inside the tube. NW growth occurred at 1130 °C in the presence of an argon flow of ∼200 mL/min for 1 h. Oxygen was supplied by ambient O_2 released from the porous alumina during growth. The NWs were converted into shorter segments in the presence of HPLC grade methanol to enhance internalization. The average NW radius and length at this point were ∼27.5 nm and ∼2.1 μm, respectively. The volumes of NWs in suspension were determined by measuring their mass with a microbalance and then dividing by the density of SiO_2 (2.6 g/cm^3). To calculate the total number of NWs, the volume was divided by the average volume of a single NW, 5.0×10^{-15} cm^3 ($\bar{R} = 27.5$ nm, $\bar{L} = 2.1$ μm).

StxA1 was purified from *E. coli* SY327(pSC25), harboring the gene encoding StxA1, using previously described methods.[15,22] Briefly, *E. coli* SY327(pSC25) log phase cells were harvested, periplasmic proteins were extracted by polymyxin B sulfate (50 μg/mL) treatment, precipitated with ammonium sulfate, dialyzed, and adsorbed to a Matrex Gel Green A agarose column (Amicon, Carrigtwohill, Ireland) equilibrated with PBS (pH 7.4). StxA1 eluted as a single peak at a concentration of ∼0.3 M NaCl using a 0.15−1.0 M NaCl gradient. Before use, the protein solution was dialyzed against 10 mM PBS; concentrations were measured with a commercial kit (Bio-Rad, Hercules, CA).

To investigate the interfacial chemistry between or among bonded Fn, StxA1, and NWs, X-ray photoelectron spectroscopy (XPS) was performed in a vacuum chamber with a base pressure of 5×10^{-10} Torr equipped with the Mg Kα emission line (1253 eV) and a hemispherical energy analyzer with a resolution of 0.025 eV. During XPS, NWs were supported on the Si substrate upon which they were grown and exposed to a 500 eV electron beam using an electron flood gun to eliminate any spurious charging of the sample. If electron neutralization of the NWs was not performed, binding energy shifts of the core level states as large as 10 eV were observed. To acquire initial spectra of noncoated NWs, the Si 2p, O 1s, and C 1s core levels were examined as previously reported.[12] The Si 2p core level of the NWs consists of a predominant peak at 103.6 eV (spectrum a, Figure 1A), which corresponds to the Si^{4+} expected for SiO_2.[23−26] Another peak is evident in this spectrum at a lower binding energy corresponding to the Si^0 of the Si(100) substrate on which the NWs were grown. The O 1s core level of the as-grown NWs is at a binding energy of 534.3 eV (spectrum a, Figure 1B). The C 1s core level of the NWs is at a binding energy of 285.5 eV (spectrum a, Figure 1C). The low signal-to-noise ratio of the C 1s core level is indicative of residual amounts of C on the surface of the NWs.

Although we previously reported[12] that the stoichiometry of the NWs used was $SiO_{2-x}C_x$, with $0.5 < x < 1.0$, in this current study, the Si 2p core level binding energy of the as-grown NWs is consistent with that of SiO_2. Taken with the low signal-to-noise ratio of the C 1s core level, we conclude that the surface stoichiometry of the NWs used in this experiment is SiO_2. The XPS studies illustrate the importance of characterizing the surface properties of the nanowires prior to performing the internalization experiments.

Our goal was to optimize StxA1 bonding to enhance intracellular StxA1 release and minimize premature release into solution. Thus, experiments were conducted to assess the effects of coating NWs with StxA1 only or in combination (added prior to or simultaneously) with Fn. To accomplish this, StxA1 (300 ng/mL) and Fn (100 nM) (Calbiochem, Darmstadt, Germany) or both were used and incubation with NWs was conducted overnight (ON) at room temperature (RT) with constant agitation. Coated NWs were washed three times with deionized (DI) water, dried in a hood, and analyzed by XPS. Coating the NWs with StxA1 resulted in a 1.4 eV shift of the Si 2p core level to a higher binding energy (Figure 1A). Subsequent coating with Fn caused a secondary shift of 0.5 eV to a binding energy of 105.5 eV. Simultaneous coating of the NWs with Fn and StxA1 resulted in a shift of 7.2 eV of the Si 2p core level to a binding energy of 110.8 eV.

Coating NWs with StxA1 resulted in no significant change in binding energy of the O 1s core level (Figure 1B). The observed spectrum is a convolution of two features: the O of the NWs (shown at a binding energy of 534.5 eV) and the O of StxA1. Subsequent coating with Fn produced a single feature (binding energy of 533.1 eV) corresponding to the O of Fn. Simultaneous coating of NWs with Fn and StxA1 produced a spectrum consisting of two features at binding energies 533.3 and 537.2 eV.

The C 1s core level of the StxA1 coating on the NWs is at a binding energy of 286.9 eV (Figure 1C). Subsequent coating with Fn resulted in a peak and a shoulder that can be deconvoluted into two features at binding energies of 286.6 and 289.5 eV, respectively. Simultaneous Fn and StxA1 coating produced a C 1s peak at a binding energy of 290.5 eV, which is attributed to a complex interaction between StxA1 and Fn. The shoulder in spectrum c of Figure 1C at a binding of 289.5 eV likely corresponds to a C 1s StxA1−Fn interfacial state arising from sequential coating of the two compounds, as opposed to a homogeneous mixing that gives rise to the single C 1s feature at 290.5 eV.

XPS results of coating NWs with StxA1 are similar to previous data for Fn in which the Si 2p core level shifted to higher binding energy, while the O 1s core level remained unchanged.[12] This suggest that both proteins bind primarily to the Si sites on the NW surface. The spectral results of coating the NWs simultaneously with Fn and StxA1 demonstrate some complex interactions between Fn, StxA1, and the NWs in the form of two peaks in the O 1s core level state in spectrum d in Figure 1B. The nature of this interaction is unclear at this time and will require further study.

To avoid complex interactions between Fn and StxA1 observed with XPS, the procedure used to functionalize the NWs for the internalization assay was to first coat with StxA1 and then with Fn. An important consideration for optimizing the interaction of StxA1 with the NWs is the polarity of the two constituents. The Si sites of the NWs are in the 4+ state (positive polarity), and StxA1 exhibits a net positive charge in neutral solution due to its isoelectric point (~8.2).[27] Consequently, the interaction between the Si^{4+} sites and StxA1 is likely to be electrostatically repulsive, which may explain the smaller shift of the Si 2p core level state with StxA1 relative to Fn in Figure 1A. To increase the binding probability between StxA1 and NW, the net charge of StxA1 was converted to negative by changing the pH of StxA1 solution to pH 9.0. In contrast with initial experiments using NWs prepared without this procedural step (results not shown), increasing the solution pH resulted in efficient and reproducible cytotoxicity results (see below).

Prior to use in experiments, NW suspensions in methanol were mixed with 500 μL of DI water, incubated at 65 °C to evaporate the methanol, and sterilized by autoclaving. To obtain NWs coated with StxA1 and Fn (NW−StxA1−Fn), NWs were processed in two steps. First, NWs in suspension (50 μL) were mixed with StxA1 in DI water (4.5 μL, previously adjusted to pH 9.0 with 0.01 N NaOH), and incubated ON at RT to generate NWs coated with StxA1 (NW−StxA1). After restoration of the NW−StxA1 suspension pH to 7.0 by adding 136.7 μL DI water, the NW−StxA1 suspension was incubated with Fn (8.8 μL) ON at RT. The pH at each step was monitored using pH indicator strips (BAKER-pHIX, J.T. Baker, Germany). Analogous NW preparations coated only with StxA1 or Fn (NW−StxA1 and NW−Fn, respectively) were obtained by omitting the incubation steps with Fn or StxA1, respectively, from the procedure described above and by adding an equivalent amount of DI water. NWs processed through the coating procedure, but with proteins omitted, were prepared as controls. The final concentrations of StxA1 and Fn in the coating suspensions were 6 μg/mL or 60 ng/mL and 100 nM, respectively.

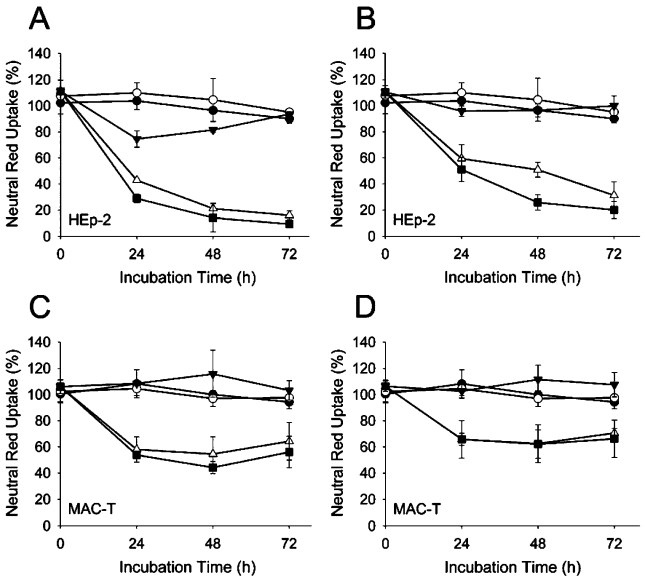

Figure 2. Cytotoxic effect of NW−StxA1−Fn complexes delivered into HEp-2 and MAC-T cells. NWs were tested at NW:cell ratios of 500:1, 1000:1, and 2000:1. NW complexes were prepared by incubating with StxA1 concentrations of 6 μg/mL (A and C) or 60 ng/mL (B and D). Except for noncoated controls, NWs were also coated with Fn (100 nM). After incubation, NR uptake was measured and compared to untreated control cultures. Data in this figure are from a representative experiment which was performed twice. (●) Noncoated NWs (2000:1). (○) NW−Fn (2000:1). (▼) NW−StxA1−Fn (500:1). (△) NW−StxA1−Fn (1000:1). (■) NW−StxA1−Fn (2000:1).

For neutral red (NR) cytotoxicity assays, MAC-T or HEp-2 cells were seeded in 96 well plates. When the cells reached 60−70% confluency, the monolayers were washed with Hank's balanced salt solution (HBSS, Gibco-BRL, NY) and the wells were filled with 190 μL of medium: low-glucose Dulbecco's modified Eagle's medium (DMEM) containing 5% fetal bovine serum (FBS) (HyClone, Logan, UT), penicillin (50 U/mL), and streptomycin sulfate (50 μg/mL) for HEp-2 cells, and high-glucose DMEM with 5% FBS, insulin (5 μg/mL), hydrocortisone (5 μg/mL), penicillin, and streptomycin sulfate for MAC-T cells. Subsequently, the cells were treated by addition of NW−StxA1, NW−Fn, or NW−StxA1−Fn suspensions (10 μL each) and incubated at 37 °C under 6% CO_2 for various lengths of time. The NW:cell ratios were 2000:1, 1000:1, and 500:1. Cells treated by addition of 200 μL of DMEM medium only were used as controls. Following incubation, the cells were washed with HBSS and stained with 200 μL of NR media (50 μg/mL of NR in DMEM medium) for 3 h, washed with 200 μL of fixative solution (1% $CaCl_2$ and 1% formaldehyde), and treated with 200 μL of 1% acetic acid in 50% ethanol solution.[28] Absorption was measured at 540 nm using an ultra microplate reader (BIO-TEK instruments, VT), and OD values were presented as percentages of cell controls.

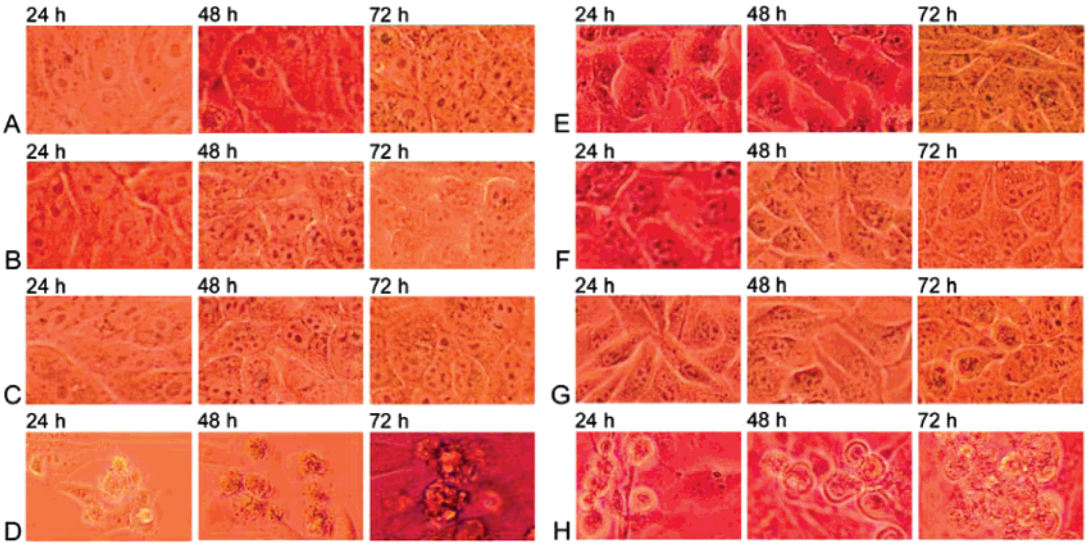

Figure 3. Microscopic images of HEp-2 (A−D) and MAC-T (E−H) cells treated with NW, NW−Fn, or NW−StxA1−Fn complexes. (A and E) Untreated cell controls. (B and F) Cells treated with noncoated NWs. (C and G) Cells treated with NW−Fn. (D and H) Cells treated with NWs−StxA1−Fn (prepared by incubating in 6 μg/mL StxA1). The NW:cell ratio was 2000:1.

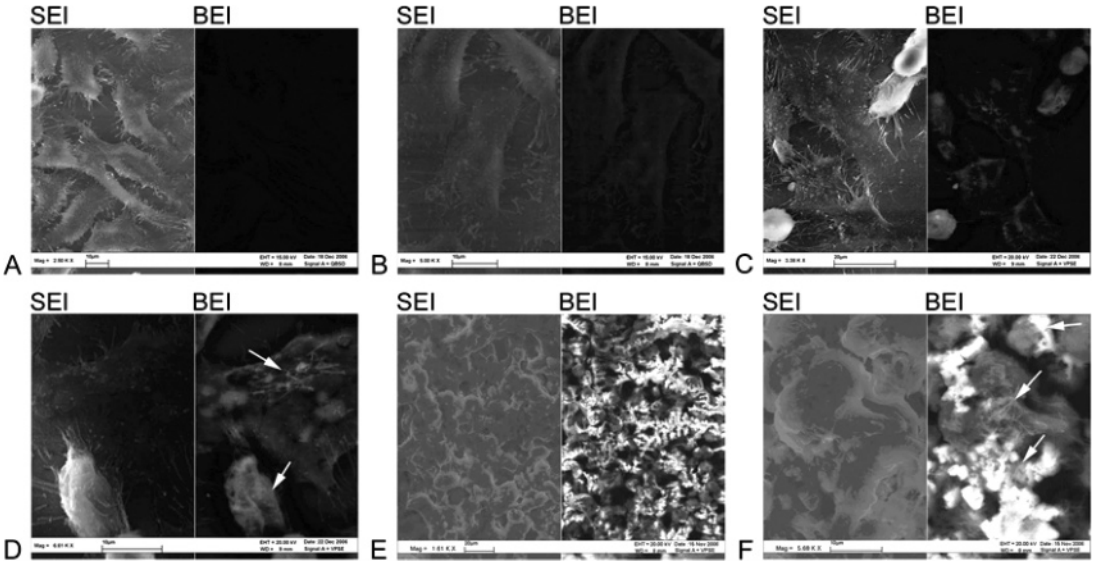

Figure 4. FESEM images of HEp-2 cells. Each image is displayed in two modes: SEI (left) and BEI (right). Cells were treated with NW−StxA1−Fn complexes (6 μg/mL StxA1) for 48 h (NW:cell ratio = 2000:1). (A and B) HEp-2 control cultures. (C and D) HEp-2 cells on the original coverslip. (E and F) Recovered detached cells. (A, C, and E) 2500×, 3380×, and 1610×, respectively. (B, D, and F) 5000×, 6610×, and 5680×, respectively.

NW−StxA1−Fn complexes produced dose- and time-dependent cytotoxicity toward both types of cultured cells (Figure 2). Exposure to NW−StxA1−Fn complexes at the relatively low NW:cell ratio of 500:1 produced results similar to cultures treated with uncoated NWs or with NW−Fn complexes. Most cells (>95%) treated with the NW or NW−Fn remained viable during the treatment. However, higher amounts of NW−StxA1−Fn (NW:cell of 1000:1 or 2000:1) produced measurable cytotoxicity within 24 h of incubation. Significantly more cytotoxicity was produced in HEp-2 compared to MAC-T cells. Although maximum NR uptake (50−60%) occurred after 24 h in MAC-T cell cultures, viability of HEp-2 cells continued to decline (to ∼10 to 20%) in cultures treatment with higher amounts of NW-StxA1-Fn (parts A and B of Figure 2). These data also demonstrate that StxA1 concentrations affect the NW coating and ultimately the level of cytotoxicity observed. Specifically, NW−StxA1−Fn prepared by incubating in a relatively low concentration of StxA1 (60 ng/mL) generated less HEp-2 NR uptake (∼80%) compared to the level (∼90%) induced by complexes incubated in higher concentrations of StxA1 (6 μg/mL).

Microscopic analysis (Nikon Eclipse TS1100, Nikon, NY) confirmed the results of NR assays (Figure 3). Cells were grown on Thermanox coverslips (Costar, Acton, MA) in 24-well plates and treated with noncoated NWs, NW−StxA1, NW−Fn, or NW−StxA1−Fn under the same condition described above. Cultures exposed to NW−StxA1−Fn had large numbers of rounded cells with a granular appearance (parts D and H of Figure 3) compared to cells with normal

morphology in untreated cultures (parts A and E of Figure 3) or cultures treated with NW controls without StxA1 (parts B, C, F, and G of Figure 3). Similar to NR assay data, MAC-T cultures had a larger number of cells with normal morphology. Because nonviable cells detach from the coverslips,[29] regions devoid of cells are readily observed in parts D and H of Figure 3.

Field emission scanning electron microscopy (FESEM) analysis confirmed NW−StxA1−Fn internalization. HEp-2 cells grown on Thermanox coverslips in 24-well plates were incubated with NW−StxA1−Fn (6 μg/mL StxA1) for 48 h as described above. Following incubation, dead detached cells were collected, transferred to, and dried onto a clean coverslip. These, the original coverslips, and coverslips from control cultures were fixed and processed for FESEM, as described previously.[12] Cell morphology observed by FESEM analysis is consistent with microscopic analysis summarized in Figure 3. The morphology of the HEp-2 control cells was elongated and attached to the coverslips, while the cultures treated with NW−StxA1−Fn were markedly different (Figure 4). Many (∼50%) of the HEp-2 cells on the coverslips and all of the detached cells were rounded (Figure 4C−F), typical of dead, dying, or apoptotic cells.[29,30]

We contrasted cultures viewed in secondary electron imaging (SEI) and backscattering electron imaging (BEI) to confirm the subsurface location of NWs in treated cultures. With SEI, the escape depth of secondary electrons is only ∼20 nm; these images provide information regarding structures at the surface and at depths of ∼≤20 nm into the cells. With BEI, the escape depth of the backscattered electrons is approximately 760 nm. Therefore, subsurface NWs designated by arrows are those that are apparent in BEI images but not with SEI. The rounding of dead cells caused an increase in their density, and therefore, they appear brighter than viable cells in the FESEM images (Figure 4C−F). In some cases, this effect interfered with the detection of internalized NWs. However, internalized NWs were apparent in cells treated with NW−StxA1−Fn but in which the brightening was not sufficient to interfere with detection (parts D and F of Figure 4). The presence of internalized NWs in cells treated with NW−StxA1−Fn, combined with cytotoxicity data described above leads to the conclusion that cytotoxicity resulted from delivery of the StxA1.

The difference in sensitivity of the HEp-2 and MAC-T cells observed by NR assays (Figure 2) and microscopic analysis (Figure 3) is noteworthy. We suspect that the reduced cytotoxicity toward the MAC-T cells is due to the hindered internalization of NW−StxA1−Fn complexes by endogenously expressed Fn. Unlike HEp-2 cells, noted for lack of Fn expression, MAC-T cells produce endogenous Fn.[14,31] Small quantities of Fn stimulate internalization of staphylococci expressing Fn-binding proteins whereas, excessive concentrations reduce the internalization.[14] We propose that, similar to effects reported for staphylococci, endogenous Fn produced by MAC-T cells compete with NW−StxA1−Fn complexes for a limited number of integrin binding sites on the cell surface.

This study showed that NWs can be used to deliver cytotoxic agents into target cells efficiently. We demonstrated this principal using StxA1 which cannot enter cells naturally without its counterpart B subunit. The potential uses of this technology include immunotherapy for various diseases such as cancer, autoimmunity, or infectious diseases. Ongoing studies include improved functionalization of NWs aimed at increasing internalization efficiency and replacing Fn with various ligands that will promote internalization by specific target cells.

Acknowledgment. This work was supported, in part, by the Idaho Agricultural Experiment Station, the National Research Initiative of the USDA Cooperative State Research, Education and Extension Service, Grant Number 04-04562 (C.J.H.), and Public Health Service grants, U54-AI-57141, P20-RR016454, and P20-RR15587 (G.A.B. and C.J.H.), and the University of Idaho-BANTech Initiative. This work was also supported by the W.M. Keck Foundation (D.N.M.) and the NSF, Grant Number EPS0132626 (D.N.M.). The authors thank Haiqing Sheng and Jie Li for the purification of recombinant StxA1.

References

(1) Emerich, D. F.; Thanos, C. G. *Biomol. Eng.* **2006**, *23*, 171−184.
(2) Rawat, M.; Singh, D.; Saraf, S. *Biol. Pharm. Bull.* **2006**, *29*, 1790−1798.
(3) Sinha, R.; Kim, G. J.; Nie, S.; Shin, D. M. *Mol. Cancer Ther*. **2006**, *5*, 1909−1917.
(4) Cuenca, A. G.; Jiang, H.; Hochwald, S. N.; Delano, M.; Cance, W. G.; Grobmyer, S. R. *Cancer* **2006**, *107*, 459−466.
(5) Jain, K. K. *Trends Biotechnol.* **2006**, *24*, 143−145.
(6) des Rieux, A.; Fievez, V.; Garinot, M.; Schneider, Y. J.; Preat, V. *J. Controlled Release* **2006**, *116*, 1−27.
(7) Couvreur, P.; Stella, B.; Reddy, L. H.; Hillaireau, H.; Dubernet, C.; Desmaele, D.; Lepetre-Mouelhi, S.; Rocco, F.; Dereuddre-Bosquet, N.; Clayette, P.; Rosilio, V.; Marsaud, V.; Renoir, J. M.; Cattel, L. *Nano Lett.* **2006**, *6*, 2544−2548.
(8) Petri-Fink, A.; Chastellain, M.; Juillerat-Jeanneret, L.; Ferrari, A.; Hofmann, H. *Biomaterials* **2005**, *26*, 2685−2694.
(9) Klumpp, C.; Kostarelos, K.; Prato, M.; Bianco, A. *Biochim. Biophys. Acta* **2006**, *1758*, 404−412.
(10) Roy, I.; Ohulchanskyy, T. Y.; Pudavar, H. E.; Bergey, E. J.; Oseroff, A. R.; Morgan, J.; Dougherty, T. J.; Prasad, P. N. *J. Am. Chem. Soc.* **2003**, *125*, 7860−7865.
(11) Kneuer, C.; Sameti, M.; Bakowsky, U.; Schiestel, T.; Schirra, H.; Schmidt, H.; Lehr, C. M. *Bioconjugugate Chem.* **2000**, *11*, 926−932.
(12) Beaux, M. F.; Wang, L.; Zhang, D.; Gangadean, D.; McIlroy, D. N.; Kwon, N. H.; Dziewanowska, K.; Bohach, G. A. *J. Biomed. Nanotechnol.* **2006**, *2*, 23−28.
(13) Sinha, B.; Francois, P. P.; Nusse, O.; Foti, M.; Hartford, O. M.; Vaudaux, P.; Foster, T. J.; Lew, D. P.; Herrmann, M.; Krause, K. H. *Cell. Microbiol.* **1999**, *1*, 101−117.
(14) Dziewanowska, K.; Carson, A. R.; Patti, J. M.; Deobald, C. F.; Bayles, K. W.; Bohach, G. A. *Infect. Immunol.* **2000**, *68*, 6321−6328.
(15) Hovde, C. J.; Calderwood, S. B.; Mekalanos, J. J.; Collier, R. J. *Proc. Natl. Acad. Sci. U.S.A.* **1988**, *85*, 2568−2572.
(16) Warnier, M.; Romer, W.; Geelen, J.; Lesieur, J.; Amessou, M.; van den Heuvel, L.; Monnens, L.; Johannes, L. *Kidney Int.* **2006**, *70*, 2085−2092.
(17) Jacewicz, M. S.; Acheson, D. W.; Mobassaleh, M.; Donohue-Rolfe, A.; Balasubramanian, K. A.; Keusch, G. T. *J. Clin. Invest.* **1995**, *96*, 1328−1335.
(18) Sheng, H.; Davis, M. A.; Knecht, H. J.; Hancock, D. D.; Van Donkersgoed, J.; Hovde, C. J. *J. Clin. Microbiol.* **2005**, *43*, 3213−3220.
(19) Sandvig, K.; van Deurs, B. *EMBO J.* **2000**, *19*, 5943−5950.
(20) Hoey, D. E.; Sharp, L.; Currie, C.; Lingwood, C. A.; Gally, D. L.; Smith, D. G. *Cell. Microbiol.* **2003**, *5*, 85−97.

(21) Wagner, R. S.; Ellis, W. C. *Appl. Phys. Lett.* **1964**, *4*, 89−90.
(22) Zollman, T. M.; Austin, P. R.; Jablonski, P. E.; Hovde, C. J. *Protein Expr. Purif.* **1994**, *5*, 291−295.
(23) Wood, R.; Hofstra, P.; Johnson, D. Optical and Eectrical Properties of Cr-SiO Thin Films for Flat Panel Displays, Luxell Technologies Inc., Figure 4. http://www.luxellresearch.com/crisio%20paper.pdf (accessed 01/22/07).
(24) C. Evans, Associates Oxide Thickness Measurements by Electron Spectroscopy for Chemical Analysis. http://www.cea.com/literature/AN-ESCA-19.pdf (accessed 01/22/07).
(25) Niederhauser, T. L.; Jiang, G.; Lua, Y.-Y.; Dorf f, M. J.; Woolley, A. T.; Asplund, M. C.; Ber ges, D. A.; Linford, M. R. A New Method of Preparing Monolayers on Silicon and Patterning Silicon Surfaces by Scribing in The Presence of Reactive Species, Figure 3. http://www.math.byu.edu/∼mdorff/Papers/DorffPaper05.pdf (accessed 01/22/07).
(26) Spadafora, M. M. Thermal Oxidation of $Si_{1-x}Ge_x$ Epitaxial Layers, Università; Degli Studi Di Catania, Figure 3.1. http://www.ct.infn.it/Matis/PDF/Spadafora-PhDThesis.pdf (accessed 01/22/07).
(27) Yutsudo, T.; Honda, T.; Miwatani, T.; Takeda, Y. *Microbiol. Immunol.* **1987**, 3*1*, 189−197.
(28) Hughes, A. K.; Stricklett, P. K.; Kohan, D. E. *Kidney Int.* **1998**, 5*4*, 426−437.
(29) Jung, Y.; Miura, M.; Yuan, J. *J. Biol. Chem.* **1996**, *271*, 5112−5117.
(30) Otto, A. M.; Paddenberg, R.; Schubert, S.; Mannherz, H. G. *J. Cancer Res. Clin. Oncol.* **1996**, *122*, 603−612.
(31) Akers, R. M.; Ellis, S. E.; Berry, S. D. *Domest. Anim. Endocrinol.* **2005**, *29*, 259−267.

NL071179F